ACS Sustainable Chemistry & Engineering
Research Article
Cite This: ACS Sustainable Chem. Eng. 2018, 6, 2942−2953
pubs.acs.org/journal/ascecg

Poly(ether sulfone) Nanofibers Impregnated with β-Cyclodextrin for Increased Micropollutant Removal from Water

Andrea I. Schäfer,[†] Katharina Stelzl,[†,‡] Maryam Faghih,[†] Soujit Sen Gupta,[‡] Kumaranchira Ramankutty Krishnadas,[‡] Stefan Heißler,[§] and Thalappil Pradeep*[,‡]

[†] Membrane Technology Department, Institute of Functional Interfaces (IFG), Karlsruhe Institute of Technology (KIT), Hermann-von-Helmholtz-Platz 1, 76344 Eggenstein-Leopoldshafen, Germany

[‡] DST Unit of Nanoscience (DST UNS) and Thematic Unit of Excellence (TUE), Department of Chemistry, Indian Institute of Technology Madras, Chennai 600 036, India

[§] Chemistry of Oxydic and Organic Interfaces Department, Institute of Functional Interfaces (IFG), Karlsruhe Institute of Technology (KIT), Hermann-von-Helmholtz-Platz 1, 76344 Eggenstein-Leopoldshafen, Germany

Supporting Information

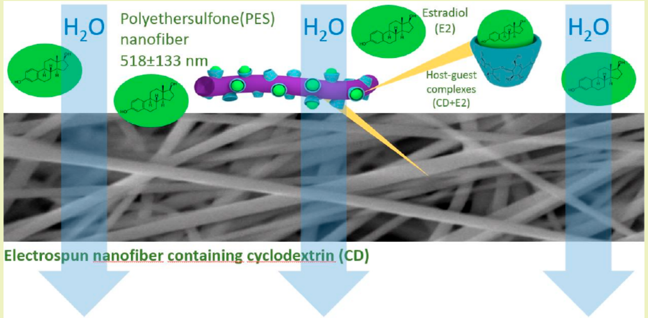

ABSTRACT: Cyclodextrin−polymer composite electrospun nanofibers were developed for micropollutant (MP) removal from water. The fibers were fabricated by electrospinning of mixed poly(ether sulfone) (PES) and β-cyclodextrin (CD) solutions under optimal conditions. The composite fibers were compared with bare PES nanofibers prepared by the same method. Scanning electron microscopy revealed that CD did not alter the fiber morphology, while the fiber capacity for MP uptake was enhanced by CD through the formation of inclusion complexes. The availability of CD on the fibers was confirmed by the emergence of visible luminescence due to the inclusion of a quantum cluster, $Au_{25}SBB_{18}$ (SBB = 4-(*tert*-butyl)benzylmercaptan in thiolate form), in the cavities of CD exposed on fiber surfaces. The steroid hormone estradiol (E2) (100 ng/L) and pesticide chlorpyrifos (CP) (5 mg/L) were used as model pollutants in batch experiments designed to measure uptake potential. The nanofibers interact strongly with the model pollutants because of their high surface area and surface affinity. Increases of 20% in E2 uptake and 80% in CP uptake compared with bare PES nanofibers were observed. This behavior indicates promising applications of CD-containing materials for MP removal in water treatment and membrane technology.

KEYWORDS: *Electrospinning, Macrocyclic host molecule, Estradiol (E2), Chlorpyrifos (CP), Adsorption, Water treatment*

INTRODUCTION

A wide range of micropollutants (MPs), composed mostly of pharmaceuticals, personal care products, and pesticides, occur in very low concentrations of a few nanograms to micrograms per liter in the water cycle. These pollutants cover a large array of chemicals, many of which are endocrine disruptors. Common endocrine disruptors are hormones, antidepressants, painkillers, personal care products, pesticides, plasticizers, and flame retardants.[1−3] While those pollutants are harmful to both the environment and wildlife in affected water bodies,[4,5] their negative effects on human health through accumulation in the food chain and contaminated drinking water cause significant economic burdens on existing water treatment methods.[6]

Conventional wastewater treatment plants cannot adequately remove a number of MPs because of the low concentrations, low molecular weights, and low biodegradability of MPs.[7] This results in the release of MPs with treated effluents[8] and affects water bodies such as lakes, rivers, and oceans.[2,3,8−11] Current treatment options for MP removal are coagulation−flocculation, activated carbon adsorption, ozonation, advanced oxidation processes, membrane filtration, membrane bioreactors, and attached -growth treatment processes.[8,12,13] Each of these technologies exhibits specific limitations such as by-product formation, inadequate removal, elevated treatment costs, or high energy requirements. Membrane filtration processes such as nanofiltration or reverse osmosis are interesting options for MP removal.[14,15] However, these processes are energy-intensive, and MP removal is typically unselective. It is hence necessary to develop new materials and composites designed for more specific MP removal. The aim of this study is to develop materials that are able to remove MPs at significantly higher water permeability than membrane processes and hence require relatively low applied pressures. This offers a process that is less energy-intensive and inexpensive.

Received: July 4, 2017
Revised: December 1, 2017
Published: December 26, 2017

ACS Publications

DOI: 10.1021/acssuschemeng.7b02214

Table 1. Characteristics of Estradiol (E2), Chlorpyrifos (CP), β-Cyclodextrin (CD), and Poly(ether sulfone) (PES)

Material	Molecular structure[a]	Molecular weight (g/mol)	Diameter (nm)	Ref.
Estradiol (E2) $C_{18}H_{24}O_2$	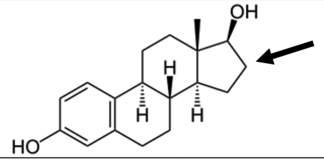	272.4	0.796	[59]
Chlorpyrifos (CP) $C_9H_{11}Cl_3NO_3PS$	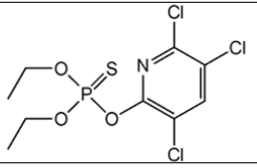	350.59	0.45	[58]
β-cyclodextrin (CD) $C_{42}H_{70}O_{35}$	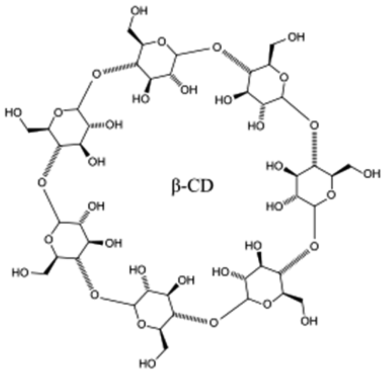	1134.98	outer: 1.53 inner: 0.78	–
Poly(ether sulfone) (PES) $[C_6H_4\text{-}4\text{-}C(CH_3)_2C_6H_4\text{-}4\text{-}OC_6H_4\text{-}4\text{-}SO_2C_6H_4\text{-}4\text{-}O]_n$	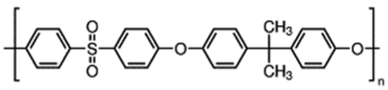	~35,000	–	–

[a] The arrow indicates the D ring of the E2 molecule, which goes into the cavity of β-CD.[60]

Even though nanofiber mats do not usually have pore sizes that are adequate for water disinfection, nanofibers are potential materials for membrane fabrication. Nanofibers have significant adsorptive properties due to their large surface areas and the possibility to incorporate specific functionalities.[16,17] Examples of such active chemistries are the inclusion of carbon nanotubes to create antimicrobial materials,[18] enzymes for catalytic reactions,[19] and the production of superhydrophobic/superoleophilic fibers for oil/water separation.[20,21] Electrospinning is the process applied to produce nanofibers from polymers with diameters ranging from tens to hundreds of nanometers.[22,23] Nanofibers can be produced from suitable polymer solutions extruded from a thin capillary while a voltage in the range of a few kilovolts is applied. Those fibers accumulate in a nonordered fashion on the collector and form a nanofiber mat,[22−26] unless a drum collector that can collect the fibers in an aligned manner is used.

Affinity membranes are one of the main types of electrospun nanofibrous membranes for the removal of specific molecules from liquids. Nanofiber affinity membranes have been made from common membrane polymers such as regenerated cellulose, polysulfone, and poly(ether sulfone) (PES) for pollutant adsorption.[17,27,28] PES is a suitable carrier polymer for water treatment applications because of its high permeability, good mechanical and thermal stability, and biocompatibility.[29,30] To enhance the adsorptive capacity and selectivity of the fibers, functional molecules may be added. Selectivity may target micropollutants over water matrix compounds present at significantly higher concentrations. A particularly popular class of molecules for this application is cyclodextrins. β-Cyclodextrin (β-CD) is a cyclic oligosaccharide formed by α-(1,4)-linked glucopyranose units,[31] with seven glucopyranose units[32,33] being suitable for a wide variety of applications.[34] The glucopyranose units form a toroidal structure with a hydrophobic inner cavity and a hydrophilic outer surface. The hydrophobic cavity enables the CD to form inclusion complexes with other guest molecules that are mainly hydrophobic in nature by means of non-covalent interactions between the guest molecule and the CD host. Mechanisms include hydrogen bonds, van der Waals forces, and electrostatic forces as well as hydrophobic and hydrophilic interactions between CD, the surrounding material, and the guest molecule.

CDs can be used as a loose adsorbent[35] or be imbedded into a membrane substrate.[36] The addition of CD was reported to increase the pure water flux and rejection of natural organic matter through membranes.[37−41] Uyar et al.[42] introduced β-CD into poly(methyl methacrylate) as well as into polystyrene fibers, and for the latter, increased adsorption of phenolphthalein as a function of β-CD content in the fibers was evident.[43] Micropollutants such as bisphenol A are adsorbed directly to the fibers with reported adsorption capacities as high as 88.7 μmol/g, and desorption is achieved by washing the fibers with ethanol. The integration of adsorption into a larger

DOI: 10.1021/acssuschemeng.7b02214
ACS Sustainable Chem. Eng. 2018, 6, 2942−2953

treatment system was anticipated to lead to more sustainable water technologies.[44]

Both hormones and pesticides are common MPs. The hormone estradiol is found in treated wastewater in the range of 1−100 ng/L[45] and has proven adverse effects on human health.[46] The cavities of CD can trap the A ring of steroid molecules and can efficiently make a host−guest complex.[47] Bednarek et al.[48] investigated the complexes of β-CD with prednisolone, ethinylestradiol, and estriol and found a model of binding based on ^{1}H NMR experiments. Nagy et al.[49] showed that CD-based sorbents can remove up to 95% of the estrogenic compounds (17β-estradiol, ethinylestradiol, and estriol). Chlorpyrifos (CP) is a common organophosphate insecticide used for protection of a variety of food and feed crops.[50,51] CP is commercialized under a variety of trade names, such as Dursban, Lorsban, Dowco 179, Pyrinex, and Coroban.[50,52] Although CP has diverse applications, it has been found that this insecticide has significant negative effects on the human nervous, respiratory, and cardiovascular systems.[53,54] Being an organophosphate, CP can be absorbed through the skin, conjunctiva, gastrointestinal tract, and lungs.[50] CP has been detected at concentrations of up to 190 ng/L in water bodies, significantly above the allowed CP concentration in the European Union,[55] set at 0.1 and 0.5 μg/L as the maximum admissible concentrations for individual and total amounts of pesticides, respectively.[56] Several studies have reported the incorporation of CD by blending in electrospinning polymer solutions or functionalization of the surface of electrospun nanofibers for adsorption of organic molecules from water and wastewater applications, as summarized in Table S1.

In this research, PES nanofibers with incorporated CD were investigated to determine (1) whether the accessibility of CD on the fiber surface for pollutant removal can be maintained, (2) whether CD enhances pollutant removal in comparison with bare PES fibers, and (3) whether the CD is stable in the nanofiber when exposed to water (in which CD is soluble).

■ EXPERIMENTAL SECTION

Pollutant Characteristics and Analysis. Radiolabeled hormones [2,4,6,7-^{3}H]β-estradiol (E2) (2.59 TBq/mmol) with an activity of 37 MBq/mL as an ethanol solution was purchased from PerkinElmer (Waltham, MA, USA). Milli-Q type-1 water (>18.2 MΩ/cm at 25 °C; Merck Millipore, Darmstadt, Germany) was used to prepare a 10 μg/L E2 stock solution. Very low concentrations of ^{3}H-labeled hormones (as low as 0.1 ng/L) were detected with a liquid scintillation counter (2550 TR/AB; Packard, Downers Grove, IL, USA).[57] For scintillation counting, 1 mL of the sample was mixed with 1 mL of scintillation liquid (Ultima Gold LLT; PerkinElmer) in a 20 mL glass scintillation vial (Wheaton, Fisher Scientific, Schwerte, Germany) Then the sample was counted in triplicate (10 min for each measurement). Calibration standards were prepared with 0, 0.1, 1, 10, and 100 ng/L E2 solutions.

The pesticide chlorpyrifos was purchased as an analytical standard (99.9% purity; Fluka Analytical, Sigma-Aldrich). A stock solution of CP was prepared in ethanol at a concentration of 1000 mg/L (the solubility of CP in ethanol is 497.07 g/L at 25 °C).[58] This solution was diluted prior to each experiment with distilled water to the desired concentration, usually 5 mg/L, a comparatively high pollutant concentration used for feasibility studies. The CP concentration was measured using gas chromatography (GC) on a Clarus 680 gas chromatograph (PerkinElmer) with an electron capture detector. CP was extracted from the aqueous solution with hexane, and 1 μL was injected into the gas chromatograph. The injector temperature was set to 200 °C. The oven temperature was initially set at 75 °C for 1 min, then increased at a rate of 20 °C/min to 150 °C, held at 150 °C for 3 min, increased at 20 °C/min to 250 °C, held at 250 °C for 2 min, increased at 20 °C/min to 300 °C, and held at 300 °C for 5 min. The total duration was 22.25 min. The hexane used for sample extractions was Chromasolv for HPLC (≥97.0% (GC); Sigma-Aldrich). Characteristics of E2 and CP are summarized in Table 1.

Fiber Preparation. The polymer used for fiber production was Veradel 3200 poly(ether sulfone) (Solvay Specialty Polymers). β-CD was purchased from MP Biomedicals LLC (Solon, OH, USA). *N*,*N*-Dimethylformamide (DMF) (>99.5%, Emparta ACS; Merck) was used as the solvent. The characteristics of PES and β-CD are summarized in Table 1. Two types of fibers were prepared: β-CD−PES composites (PES+CD) as well as pure PES without added CD (PES). A PES spinning solution containing 25 wt % PES with DMF as the solvent was prepared. For the CD-doped fibers (PES+CD), 10 wt % β-CD with respect to the polymer weight was added to the spinning solution.

The nanofibers were prepared by electrospinning (ESPIN-NANO; PECO-Chennai, India). The fibers were spun from a spinneret needle with an outer diameter of 0.4 mm at 25 kV onto an aluminum sheet substrate placed on a drum collector (PECO-Chennai) rotating at 2500 rpm. The syringe pump extruding the spinning solution was set to a flow rate of 0.3 mL/min, and the distance from the needle tip to the drum collector was 20 cm. After electrospinning, the aluminum sheet holding the fibers was removed from the drum collector, and the fiber mat could be peeled off the substrate for analysis.

To prepare samples for transmission electron microscopy (TEM), a few fibers (spinning time ≈ 1 s) were spun directly onto stationary TEM grids, with all of the other spinning parameters being the same as for preparing the fiber mats. For hyperspectral imaging (HSI), a small number of fibers were spun directly onto HSI glass slides for single-fiber analysis.

Fiber Static Adsorption in Waters Containing Estradiol. Static adsorption experiments were performed using radiolabeled [2,4,6,7-^{3}H]β-estradiol (2.59 TBq/mmol). Different masses of fibers were put in conical shaker flasks (250 mL; Duran Group, Wertheim, Germany) containing 100 mL of 100 ng/L E2 solution, and the flasks were placed in an incubator shaker (Innova 43 R; New Brunswick Scientific, Edison, NJ, USA) at 260 rpm and a constant temperature of 20 °C. A metal paper clip was attached to each nanofiber sample to prevent nanofiber floating. It should be noted that adsorption on glass surfaces (<0.7%) and paper clips was negligible during long-term tests with hormone solution. Then 2.5 mL samples were taken with 5 mL pipettes at certain time intervals, assuring that no nanofiber was removed during the sampling procedure. The sampling periods were 0, 0.1, 0.25, 0.5, 1, 3, 5, 7, 9, 24, 26, 48, 72, and 96 h. The percentage of hormone removal was calculated using eq 1:

$$\%\text{ hormone removal} = \frac{c_0 - c_t}{c_0}\cdot 100 \tag{1}$$

where c_0 (in ng/L) is the initial concentration and c_t (in ng/L) is sample concentration at time *t*.

Fiber Adsorption and Desorption Studies in Waters Containing CP. CP adsorption experiments were performed using a batch process wherein 3 mg of fiber was added to 100 mL of aqueous CP solution with a concentration of 5 mg/L. After an equilibration time of 12 h, the concentration of the solution was determined by GC. The aqueous CP solution was freshly prepared for every batch to minimize hydrolysis of CP.

To determine desorption or adsorbent recovery, the fibers were washed multiple times with water and measured after every washing step. Small amounts (∼1 mg) of fibers were soaked in 100 mL of 1000 mg/L CP stock solution overnight to reach equilibrium. After removal from the solution, 3 mL of deionized water was added, and the samples were placed on a shaker for 15 min. This washing step was repeated one to four times. After washing, the samples were air-dried and stored in a desiccator until analysis by infrared absorption spectroscopy. Samples were analyzed using a UV−vis spectrometer at 205 nm to determine desorption of CP to ethanol. Optical absorption spectroscopy was performed with a PerkinElmer Spectrum One instrument in the wavelength range of 190−1100 nm.

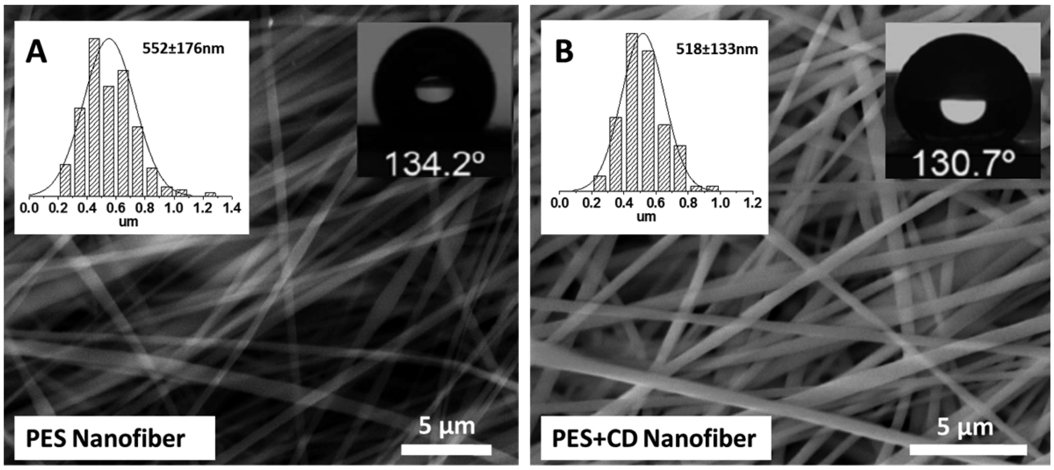

Figure 1. SEM images of (A) PES nanofibers (average fiber diameter of 552 ± 176 nm) and (B) PES+CD nanofibers (average fiber diameter of 518 ± 133 nm).

FIBER CHARACTERIZATION

Scanning Electron Microscopy. Scanning electron microscopy (SEM) images were taken on a Quanta 200 instrument (FEI, Hillsboro, OR, USA) with a 30 kV electron beam to analyze the morphology of the nanofibers.

Brunauer−Emmett−Teller Analysis. Brunauer−Emmett−Teller (BET) theory-based surface analysis was performed on fiber samples containing CD as well as fibers without CD (pure PES fibers) to determine the specific surface areas of the fibers. For surface analysis, 208 mg of PES+CD fibers and 203 mg of PES fibers were removed from their aluminum substrates and outgassed at 100 °C under vacuum for 12 h before the BET measurements were started. The nitrogen adsorption was measured on an ASAP 2020 porosimeter (Micromeritics, Norcross, GA, USA).

Contact Angle Measurements. The water contact angles of the electrospun nanofibers were measured using the sessile drop technique (DSA 25; Kruss, Hamburg, Germany) at room temperature. Milli-Q water was used as the probe liquid, and the contact angle was measured at 1 s intervals. Each time a 6 μL drop was used, and measurements were performed for 10 s. The average of five measurements at each interval was reported as the contact angle for each sample.

Hyperspectral Imaging of Fibers Coated with $Au_{25}SBB_{18}$ Gold Nanoclusters. A hyperspectral imaging system (CytoViva Inc., Auburn, AL, USA) was used for fluorescence imaging of the fibers. The nanofibers were spun directly onto HSI glass slides and dipped into the $Au_{25}SBB_{18}$ (SBB = 4-(*tert*-butyl)benzylmercaptan in thiolate form) cluster solution for 15 min at room temperature. Subsequently, the fibers were dipped in clean hexane to remove the nonadsorbed clusters, and a single fiber was analyzed under white and fluorescent light to compare the fluorescence intensities of the two fiber types.[61]

Clusters composed of a few atoms of noble metals protected with ligands belong to a new class of materials with properties (in this case intense luminescence) very different from those of the bulk materials.[62] Organic-soluble Au_{25} clusters protected with molecules such as phenylethanethiol (PET) and glutathione (GSH), with molecular formulas $Au_{25}PET_{18}$ and $Au_{25}SG_{18}$, are examples of this class of materials. CD cavities can be used as suitable hosts to create host−guest chemistry for these materials.[61,63] The clusters used here were composed of a core containing 25 gold atoms protected by 18 SBB molecules. The interactions of these clusters with β-CD and their red luminescence when excited with fluorescent light (480−510 nm) have been reported by Mathew et al.[64] The clusters form inclusion complexes with the CD molecules through the host−guest interaction between the soluble SBB and the CD cavity. Hence, the abundance of CD cavities on the fiber surfaces can be visualized.

Transmission Electron Microscopy and Energy-Dispersive Spectroscopy. TEM imaging and energy-dispersive spectroscopy (EDS) analysis were performed using a JEOL 3010 high-resolution transmission electron microscope (JEOL, Tokyo, Japan). Nanofibers were spun directly onto copper grids for TEM analysis. Single fibers were imaged, and EDS mapping of the elements carbon, sulfur, phosphorus, and chlorine was performed for both fiber types after exposure to CP.

Attenuated Total Reflectance Fourier Transform Infrared Spectroscopy. Attenuated total reflectance Fourier transform IR (ATR-FTIR) spectra were measured using a Bruker Tensor 27 FTIR spectrometer (Bruker Optics, Ettlingen, Germany) equipped with a room-temperature deuterated glycinesulfate (RT-DTGS) detector and a Bruker Platinum ATR accessory (diamond crystal with one reflection). All of the spectra were recorded at room temperature (22 °C). Bruker OPUS 7.2 software was used for measurements as well as spectral evaluation. Spectra were recorded from 4000 to 370 cm^{-1} with a spectral resolution of 4 cm^{-1} against an air background. In each measurement, 32 scans were coadded, and a baseline correction was performed after the measurement. Spectra were measured for both the fiber types before and after CP adsorption.

Simultaneous Thermal Analysis Mass Spectrometry with Thermogravimetry/Differential Scanning Calorimetry. Simultaneous thermal analysis (STA) was performed with a STA 449 C Jupiter (Netzsch-Gerätebau GmbH, Selb, Germany) equipped with a thermogravimetry/differential scanning calorimetry (TG-DSC) sample holder. The STA instrument was connected by a heated quartz glass capillary to a 403 C Aëolos quadrupole mass spectrometer (InProcess Instruments (IPI)/Netzsch-Gerätebau GmbH). Samples were heated from 35 to 590 °C at 10 K/min in a streaming nitrogen (50 mL/min)/nitrogen (20 mL/min) atmosphere. Conventional Al crucibles with lids were filled with sample material (0.3−4 mg). An empty Al crucible with lid served as the reference.

RESULTS AND DISCUSSION

Fiber Morphology. SEM imaging was carried out to analyze the fiber morphology and structure. The images in Figure 1 show the similarity of the PES and PES+CD fibers. Both samples show uniform and straight fibers with very few beads. The fiber diameters have a relatively narrow distribution. The average fiber diameters for the PES and PES+CD fibers were measured to be 552 ± 176 and 518 ± 133 nm, respectively. The slightly lower average fiber diameter for PES+CD fibers is attributed to weak intermolecular interactions between CD and PES and the lower viscosity of the electrospinning solution compared with that for bare PES.[43]

It has been found that addition of CD to different polymeric matrixes leads to narrower fibers.[42,65−67]

Fiber Surface Area, Length, and Volume. The length (l) and surface area (A) of the fibers can be estimated from the average fiber diameter (d) from SEM results and the density of bulk PES (ρ = 1.37 g/cm^3).[68] With the assumption of a cylindrical fiber shape, inserting the equation for the cylinder volume (V) and relating the mass (m) to the volume using the density results in eq 2:

$$V = \frac{m}{\rho} = \frac{\pi d^2 l}{4} \tag{2}$$

This can be rearranged to give the fiber length per unit mass (l/m) as

$$\frac{l}{m} = \frac{4}{\rho \pi d^2} \tag{3}$$

Since $l \gg d$, the surface areas of the fiber ends can be neglected. The surface area (neglecting the fiber ends) per unit mass is then given by eq 4:

$$\frac{A}{m} = \frac{d\pi l}{m} = \frac{4}{\rho d} \tag{4}$$

The fiber diameters measured by SEM and the calculated fiber lengths and surface areas per unit mass are given in Table 2.

Table 2. Fiber Lengths and Surface Areas (Per Unit Mass) Estimated by Assuming a Cylindrical Fiber Shape

nanofiber	average fiber diameter from SEM (nm)	fiber length (m/mg)	cylinder surface area (m^2/g)	BET surface area (m^2/g)
PES	552	3050	5.3	52
PES+CD	518	3464	5.6	31

Comparing the geometrically determined surface areas based on SEM measurements with those determined by BET analysis shows that the BET results are a factor of 10 higher, while the results compare well with reported literature values of 9−51 m^2/g for average fiber diameters of 167−2737 nm.[69] The lower estimated surface area based on geometry compared with the BET results has two possible explanations: (1) the PES fibers have a lower density than the assumed bulk polymer density because of pore formation and other effects occurring during the electrospinning process, resulting in a greater length of fibers for a given weight and fiber diameter and hence increasing the apparent specific surface area; (2) the calculation assumes that the fibers have a smooth surface, but in fact solvent evaporation from the fiber surface during electrospinning results in a rough surface and consequently an increased surface area. No significant difference in surface area between the nanofibers with and without CD could be determined.

Water Contact Angle of Nanofibers. The contact angle determines the hydrophobicity of a surface. The contact angles were found to be 134.2° and 130.7° for PES and PES+CD nanofibers, respectively. Because the outer surface of CD is hydrophilic, the decreased contact angle of the PES+CD sample compared with the PES sample can be attributed to the hydrophilic nature of CD molecules on the surface of the nanofibers.

CD Host−Guest Complexes on Fiber Surfaces. Hyperspectral imaging was used to verify the presence of CD molecules on the fiber surface and their availability for inclusion complex formation. HSI was performed on single nanofibers after immersion of the fibers into a gold cluster solution. The $Au_{25}SBB_{18}$ cluster displays red luminescence,[64] which can be detected on a fiber via HSI. Figure 2 clearly shows the increased bright-red luminescence of the PES+CD nanofiber after cluster coating (Figure 2D) compared with the PES fiber (Figure 2C). The white-light images (Figure 2A,B) confirm that the fibers had similar thickness and visibility. The inset in Figure 2C shows the PES fiber after an exposure time of 2.89 s, almost 3 times longer than the exposure time of 1.09 s used for the PES+CD fiber in Figure 2B,D. In the inset, the faint luminescence of the free cluster can be observed. Shibu and Pradeep[63] reported that gold clusters display increased luminescence when trapped in molecular cavities, such as the β-CD cavity. The much-higher luminescence exhibited by the CD-containing fibers compared to the non-CD-containing fibers can be attributed to the greater numbers of clusters attached to the fibers and the enhanced luminescence of the clusters in host−guest complexes with CD. The uniform distribution of cyclodextrin is obvious in Figure 2D. This result is in agreement with contact angle results and confirms the availability of CD for complex formation on the fiber surface.

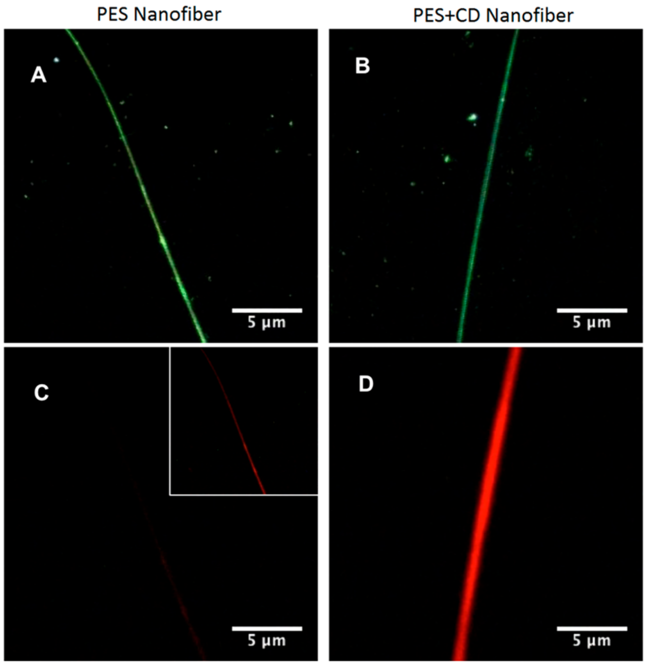

Figure 2. Hyperspectral images of individual PES nanofibers soaked in an $Au_{25}SBB_{18}$ solution: (A, C) PES nanofiber and (B, D) PES+CD nanofiber illuminated with (A, B) white light or (C, D) light with a wavelength of 480−510 nm. The fluorescence images in (C) and (D) were taken with an exposure time of 1.09 s. The image in the inset of (C) was taken with an exposure time of 2.89 s to capture the low fluorescence (more clearly visible in the bottom portion of the image).

Hormone Adsorption. CD molecules can form host−guest complexes with variety of organic molecules and MPs. Static adsorption of the hormone E2 was determined with two nanofiber samples. Figure 3 shows the E2 removal and adsorption capacity as a function of nanofiber mass after 96 h (100 mL of 100 ng/L E2 solution at 20 °C, 260 rpm, no

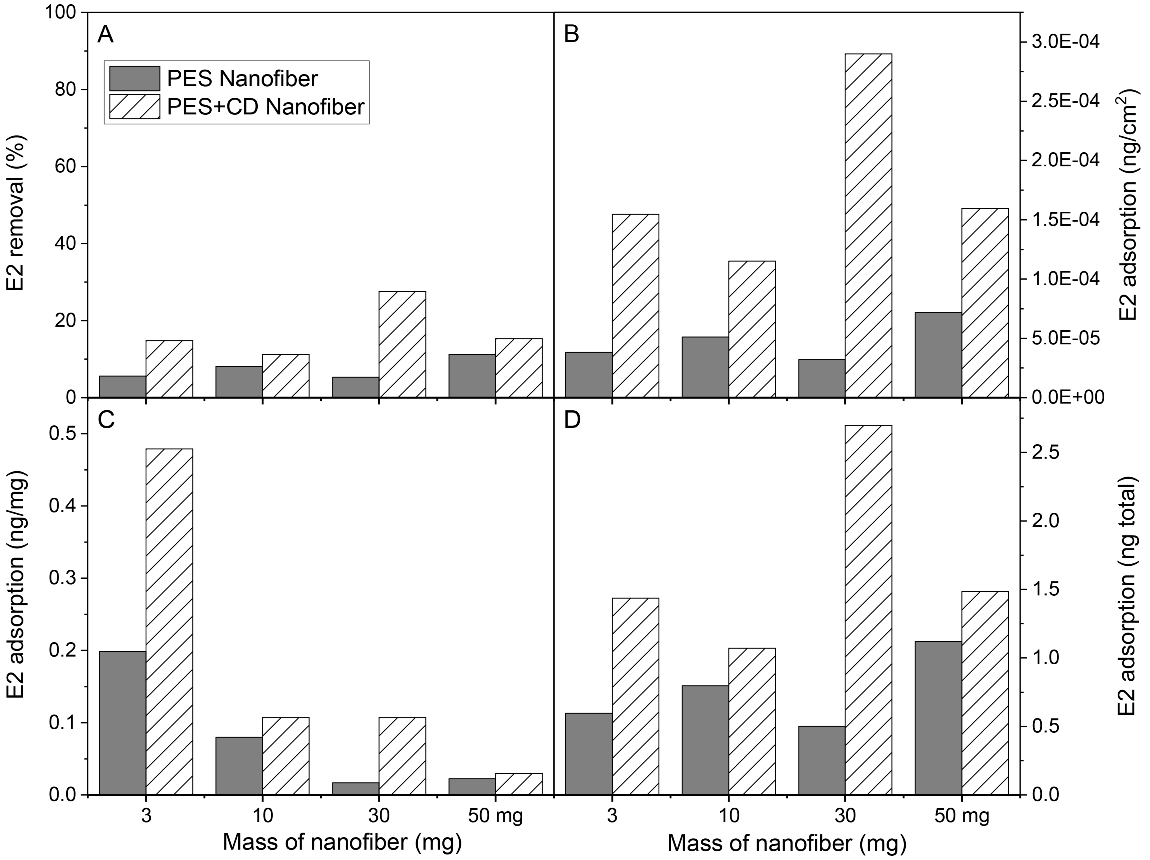

Figure 3. Estradiol (E2) adsorption on four different masses of PES and PES+CD nanofibers after 96 h: (A) percentage of E2 removal, (B) E2 mass adsorbed/nanofiber surface area determined from BET, (C) E2 mass adsorbed/mg of nanofiber, and (D) total E2 mass adsorbed on each sample.

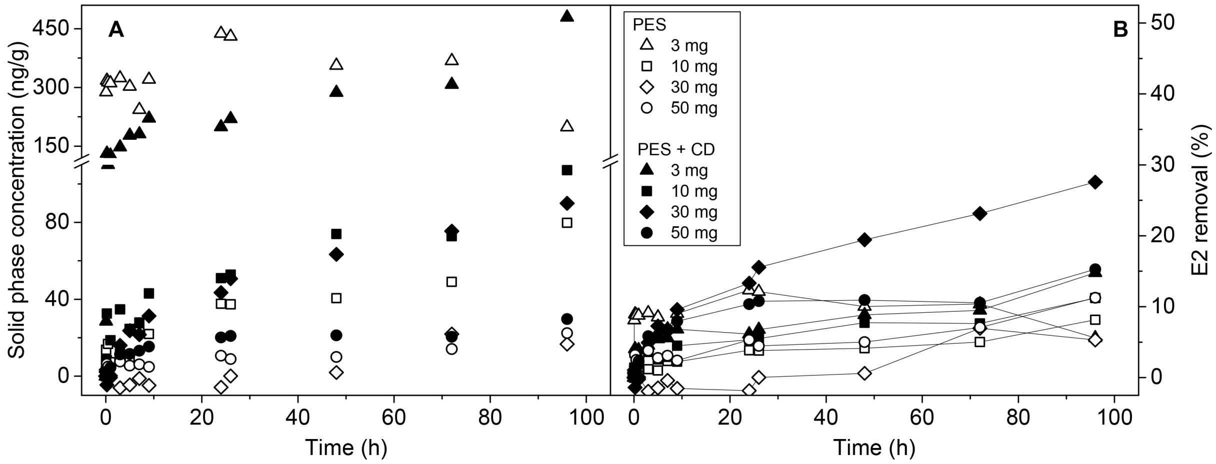

Figure 4. Static adsorption of estradiol (E2) on PES and PES+CD nanofibers as a function of time and nanofiber mass: (A) adsorbed E2 concentration per gram of fiber mat and (B) percentage of E2 removal. Conditions: 100 mL of 100 ng/L E2 solution (initial E2 mass = 10 ng) with different masses of PES nanofiber (with and without CD), 20 °C, 260 rpm, no background electrolyte. Fitting with first- and second-order kinetic models is shown in Figure S1.

background electrolyte). PES+CD fibers can adsorb a higher amount of E2 compared with bare PES nanofibers, despite the lower surface area of the nanofibers based on BET results (31 vs 52 m^2/g). The adsorption capacity increased from (3.2 to 3.7) × 10^{-5} ng/cm^2 for PES nanofibers to (11.5 to 29) × 10^{-5} ng/cm^2 for the PES+CD nanofibers. The 30 mg PES+CD sample showed the highest E2 removal (up to 27.6%), which is 22.3% more than the bare PES nanofibers. Even though nanofibers with CD showed higher E2 adsorption, increasing the nanofiber mass did not always lead to an increase in the mass of adsorbed E2. This may be due to (1) experimental error, as for the 3 mg fiber mat the amount of CD was simply not sufficient to allow determination of the difference in adsorption; (2) dissolution of CD in the fiber matrix; or (3) a nonhomogeneous dispersion of the CD molecules in the PES +CD samples. Equally, adsorption on nanofibers without CD (PES nanofibers) did not increase consistently, which could be due to variations in the quality of fiber mats and experimental error.

Figure 4A shows the time-dependent solid-phase concentration of E2 (expressed as the mass of E2 per gram of fiber), and the E2 uptake by the fiber in the form of removal percentage is shown in Figure 4B. Fitting with first- and second-order kinetic models is shown in Figure S1 and Table S2. The solid-phase concentrations are highest for the smallest amount of fiber used (3 mg) both with and without CD, suggesting that the studied adsorption did not depend on the availability of the adsorbent and that the number of fiber adsorption sites generally exceeded the number of adsorbed E2 molecules. With low masses of adsorbents (3 and 10 mg), the difference in E2 adsorption between nanofibers with and without CD is insignificant because diffusion and availability of sites control the rate of adsorption, i.e., the rate is governed by the collision frequency between E2 and PES/PES+CD. With higher adsorbent masses (30 and 50 mg), E2 removal in the presence of CD is generally higher than without CD. The difference between low and high adsorbent masses arose because the effect of diffusion was less important for the latter and CD facilitated the adsorption of E2. Nevertheless, more study is required to optimize the adsorption capacity of these materials under diverse filtration conditions.

Stability of CD in the Nanofibers. In order to study the stability of CD molecules in the electrospun nanofibers, thermal analysis mass spectrometry was performed. Figure 5 shows the TG curves with arbitrary units (a.u.) for PES and PES+CD nanofibers before and after E2 adsorption as well as for bare PES polymer and CD powder. The mass loss between 225 and 400 °C is associated with peaks in the MS curve at $m/z = 18$ (H_2O) and $m/z = 44$ (CO_2) in Figure 6, which revealed the presence of CD molecules in the samples. The small shift in the curves is caused by different net weights. The signal of PES +CD nanofibers showed the decomposition of β-CD, and the abundance of β-CD in the material was estimated as 7.2 wt %. The difference between the percentage of CD in the PES+CD nanofibers determined by TG (7.2 wt %) and the initial concentration of CD in the electrospinning solution (10 wt %) indicates potential errors and variability of CD dispersion in the nanofibers. After E2 adsorption (96 h), the PES+CD nanofibers showed a mass loss of 6.7 wt % relating to the remaining amount of CD in the fiber. The decrease in the amount of CD after adsorption may be due to the fact that CD was not cross-linked with the polymer and the water solubility of CD may cause partial release. In consequence, further work is required to cross-link β-CD with the fiber polymer. Furthermore, as the results of static adsorption revealed, different mass losses might be due to inhomogeneous dispersion of CD molecules in the electrospun nanofiber. All four samples showed similar decomposition of PES at about 475 °C, which is combined with the release of H_2O ($m/z = 18$), CO_2 ($m/z = 44$), and SO_2 ($m/z = 64$, data not shown) in Figure 6. The presence of CD in the electrospun matrix after 24 h of shaking in Milli-Q water was verified (Figures S2 and S3).

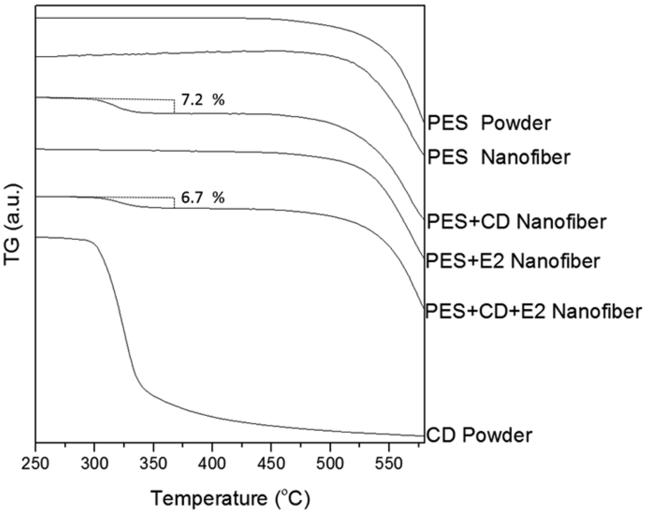

Figure 5. TG curves of pure PES powder, PES and PES+CD nanofibers before and after static adsorption in 100 mL of 100 ng/L E2 solution at 260 rpm and 20 °C, and pure CD powder. The mass loss was normalized to 100%.

Adsorption of Chlorpyrifos. CP removal from an aqueous solution was measured, and a consistently higher amount of CP was removed by the fibers containing CD (see Figure 7). The variation in the total adsorption of CP on the fibers can be explained by both variations in the fiber mats and CP analytical error. Small variations in the diameter of the fibers will result in variation in the available surface for adsorption. However, the higher adsorption for the CD-containing fibers in all of the experiments indicates that CD does increase the adsorption capability of the fibers for CP. On average, the adsorption for PES+CD fibers is 81% or 0.03 mg/mg higher compared with the non-CD fibers, confirming the results obtained with E2 at a significantly higher concentration.

Detection of CD and CP on Fibers through Elemental Analysis. TEM-EDS was used to visualize the increased adsorption of CP on the fiber surface with both fiber types (PES and PES+CD nanofibers). Both fiber types were drop-coated with CP solution on TEM stationary grids and carefully washed with distilled water. Results for the elements carbon, phosphorus, sulfur, and chlorine are shown in Figure 8. While both fibers show significant amounts of carbon and sulfur (stemming from the background as well as the PES fiber material itself), the CD-containing fiber displays higher amounts of chlorine and phosphorus on the fiber surface, indicating the increased presence of CP on that fiber.

The adsorption of CP by the nanofibers could be confirmed via several methods. TEM-EDS mapping clearly showed increased concentrations of chlorine and phosphorus on the CD-containing fibers compared with the fibers without CD (Figure 8).

Quantification of CP on Fiber Surfaces by ATR-FTIR Spectroscopy. The presence of CP on the fiber surfaces was further evidenced using ATR-FTIR spectroscopy. The IR spectrum of CP is shown in Figure S4. A peak at 964 cm^{-1} was clearly visible in both spectra after CP adsorption (see Figure 9). This peak is characteristic of P=S stretching and cannot be observed in the spectra of fibers before CP adsorption. Hence, this stretching band indicates the presence of CP on the fiber surface.[70]

The increased adsorption of CP by the PES+CD fibers, as indicated by the area under the P=S stretching band of CP (Figure 9), shows that CD is available on the fiber surface for adsorption and that the CD molecules enhance capture of CP from the solution. Comparisons of IR bands for CP and PES found in the literature and in the measured samples along with the spectrum of CP are included in the Supporting Information (Tables S3 and S4 and Figure S4). To semiquantitatively

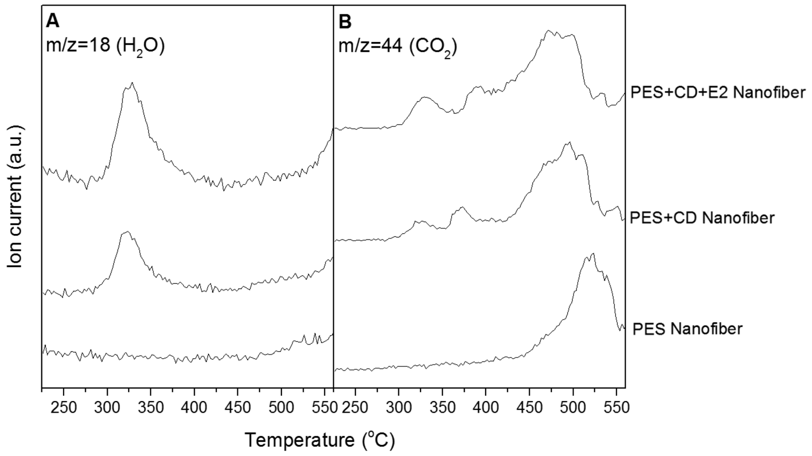

Figure 6. MS curves of (A) H_2O (m/z = 18) and (B) CO_2 (m/z = 44) of PES and PES+CD nanofibers and PES+CD nanofiber after static adsorption of E2 (PES+CD+E2 nanofiber).

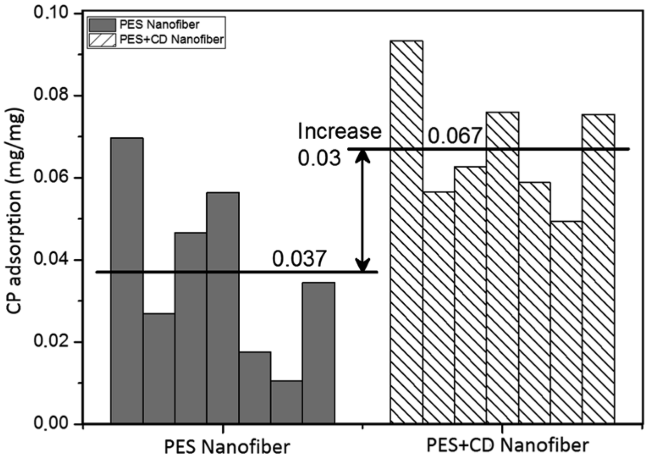

Figure 7. Adsorption of CP by PES and PES+CD nanofibers, including average values.

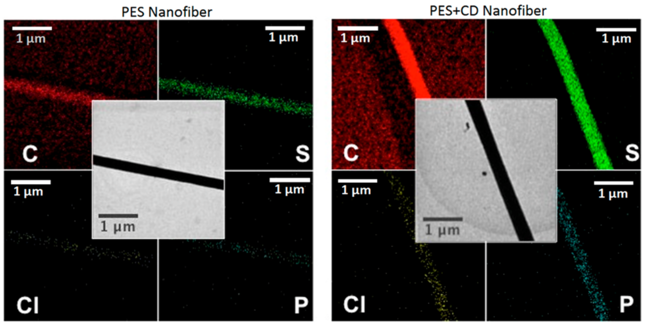

Figure 8. TEM and EDS mapped images of PES and PES+CD fibers after application of CP solution and washing with hexane. The TEM images are shown at the center. Individual elemental maps are shown around the TEM images for carbon, phosphorus, sulfur, and chlorine. The scale bars for the TEM and elemental images are identical.

determine the amount of CP adsorbed and consequently distinguish between specific adsorption to the CD and unspecific sorption to PES, the peak area was integrated from 930 to 980 cm^{-1} (as shown by the yellow region in Figure 9). It can be seen that the amount of CP adsorbed by the PES+CD fibers (4.53 a.u.) is more than 3 times greater than the amount adsorbed by bare PES fibers (1.40 a.u.). The areas are given in arbitrary units and were measured under identical conditions. The significant increase in the adsorption of CP on PES+CD nanofibers is in agreement with the results of GC analysis shown in Figure 7. It should be noted here that the identification of CP was possible because of the relatively high concentration (5 mg/L).

Determination of Sorption Reversibility. To determine the reversibility of sorption, several samples were soaked in 3 mL of water and shaken for 15 min. The washing with water showed no significant reduction in CP concentration on the fibers for either the PES or the PES+CD fibers (see Table 3). Each sample was measured four times, and the average was calculated. For both fiber types, samples after one, two, three, and four washing steps were prepared. The CP concentration differences (based on band area) between the washing cycles are not significant. These results indicate that CP adsorption by the fibers is stable in water, meaning that CP sorption will not be reversed by water.

Subsequently, desorption of CP was investigated by washing the fibers with ethanol, given that CP has a very high solubility in ethanol (497 g/L at 25 °C).[58] Desorption was measured via UV−vis spectroscopy at 205 nm. The results in Figure 10 confirm that ethanol can recover CP, allowing the fibers to be reused multiple times. This enables use of the fibers in membrane applications, where large adsorption volumes and high recovery of adsorbents are required.

While the desorption of CP from the fibers with ethanol was enhanced, the fiber morphology changed significantly after several adsorption−desorption cycles, which may be attributed to the repeated contact of PES with ethanol (Figure 11). Because ethanol is not a good solvent for PES, dissolution of the nanofibers is unlikely. The porous structure of the nanofibers may allow the ethanol molecules to penetrate the nanofiber pores. Consequently, several ethanol washing cycles may alter the fiber morphology, leading to swelling and collapse of the structure and ultimately the effectiveness of the adsorption process.

In summary, the proof of concept of incorporating CD into polymeric nanofibers for the removal of micropollutants has been demonstrated using examples such as estradiol and chlorpyrifos. Future work will focus on elucidating the interaction mechanisms, uptake kinetics, and ultimately the performance of such materials in real water. Further, micropollutants and their interactions with different types of CD will be investigated to understand the specificity in the CD−

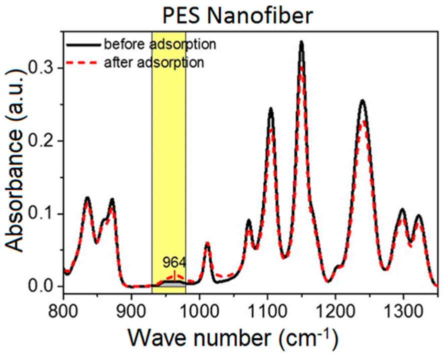

Figure 9. IR absorption spectra of PES and PES+CD nanofibers before and after adsorption. The yellow area shows the integration boundaries, and the label (964 cm^{-1}) indicates the measured P=S stretching of CP.

Table 3. Summary of Masses of the Fiber Samples and Areas of the Peak at 964 cm^{-1} after Different Washing Cycles with Water Attempting To Remove CP

sample	mass of nanofiber (mg)	no. of washing cycles	band area (a.u.)	absorbance per mg of fiber (a.u.)
PES nanofiber	1.35	1	1.601	1.18
	0.93	2	2.110	2.27
	1.02	3	2.040	2.00
	1.28	4	1.690	1.32
PES+CD nanofiber	0.65	1	3.891	6.03
	0.55	2	2.320	4.20
	1.27	3	2.219	1.74
	0.37	4	2.445	6.70

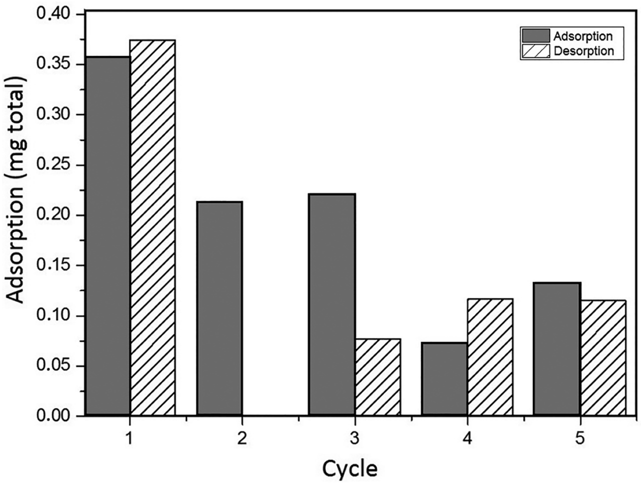

Figure 10. Adsorption−desorption performance during five cycles with CP and ethanol. Desorption was not measured for cycle 2.

micropollutant interaction. The ideal solvent for regeneration of the CD will be determined, and the operational conditions will be evaluated. Perhaps most significantly, the luminescence of the CD fibers treated with gold clusters opens up new paths for the use of these fibers in sensing applications. The methodology applied in this work to enhance the detection of available CD showed high sensitivity of gold clusters in detecting the CD cavities. By further research on this functionality of the clusters and CD, especially on the fiber surface, the production of highly selective and sensitive sensors in the nanoscale could be possible.

■ CONCLUSIONS

A method to prepare nanofibers with enhanced micropollutant adsorption capability has been developed. The enhanced abilities of poly(ether sulfone) (PES) electrospun nanofibers with cyclodextrin (CD) to form host−guest complexes with estradiol (E2) and the pesticide chlorpyrifos (CP) were evidenced. Removal of E2 and CP from aqueous solution by nanofibers without CD was compared with that by 10 wt % CD fibers. Several analytical methods were used to characterize the nanofibers and evidence MP−fiber interactions.

Adsorption of E2 increased by about 20% at a concentration of 100 ng/L for PES+CD samples, indicating the formation of a host−guest complex between the CD molecule and E2. CP adsorption at 5 mg/L increased by about 80%. Desorption of CP from the fibers was possible with ethanol, allowing fiber reuse. On the basis of the results obtained with CP and E2, it appears that a number of micropollutants will be capable of forming host−guest complexes with CDs. The β-CD used in this study may be replaced with α- or γ-CD to accommodate smaller or larger molecules, while a cross-linker would be capable of preventing the CD molecules from leaching into water.

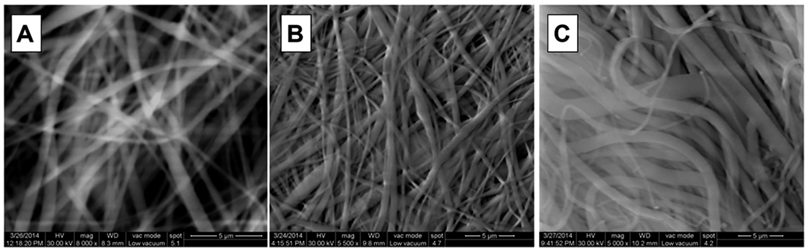

Figure 11. SEM images of fibers after (A) initial adsorption, (B) one adsorption−desorption cycle, and (C) five adsorption−desorption cycles.

DOI: 10.1021/acssuschemeng.7b02214
ACS Sustainable Chem. Eng. 2018, 6, 2942−2953

■ ASSOCIATED CONTENT

Supporting Information

The Supporting Information is available free of charge on the ACS Publications website at DOI: 10.1021/acssuschemeng.7b02214.

> S1: Summary of previous studies on incorporation of CD to electrospun nanofibers for adsorption of organic molecules (Table S1); S2: modeling of adsorption kinetics using first- and second-order kinetic models (Table S2 and Figure S1); S3: TG curves of PES and PES+CD nanofibers after 24 h in Milli-Q water (Figure S2); S4: MS curves of CO_2 ($m/z = 44$) (Figure S3); S5: comparison of IR bands in the literature with measured samples for CP (Table S3) and PES (Table S4); S6: IR spectrum of CP (Figure S4) (PDF)

■ AUTHOR INFORMATION

Corresponding Author

*E-mail: pradeep@iitm.ac.in.

ORCID

Andrea I. Schäfer: 0000-0002-7019-0327

Thalappil Pradeep: 0000-0003-3174-534X

Notes

The authors declare no competing financial interest.

■ ACKNOWLEDGMENTS

The Department of Science and Technology (DST), Government of India, is thanked for continuous financial support of the research program on nanomaterials. The Helmholtz Association is acknowledged for funding of the Membrane Technology Department through the Rekrutierungsinitiative at KIT. At IIT Madras, the authors thank Ammu Mathew for the $Au_{25}SBB_{18}$ clusters, Vidhya Subramanian for HSI measurements, Anirban Som for TEM measurements, Sundar Rajfor SEM imaging, and Mohd Azhardin Ganayee and Jeseentha Rani for help with electrospinning. At KIT, the authors thank Peter Weidler for fruitful discussions of the TEM data, Katja Emmerich and Annette Steudel for STA-MS/TG-DSC analysis and data interpretation, Matteo Tagliavini for instruction with hormone static adsorption methodology, Sahana Sheshachala for contact angle measurements, Minh Nguyen for kinetics modeling and editing, and Bryce Richards for proofreading and enhancing the section on characterization.

■ REFERENCES

(1) Nowack, B.; Bucheli, T. D. Occurrence, behavior and effects of nanoparticles in the environment. *Environ. Pollut.* **2007**, *150* (1), 5−22.

(2) Schwarzenbach, R. P.; Escher, B. I.; Fenner, K.; Hofstetter, T. B.; Johnson, C. A.; von Gunten, U.; Wehrli, B. The Challenge of Micropollutants in Aquatic Systems. *Science* **2006**, *313* (5790), 1072−1077.

(3) Tijani, J.; Fatoba, O. O.; Petrik, L. F. A Review of Pharmaceuticals and Endocrine-Disrupting Compounds: Sources, Effects, Removal, and Detections. *Water, Air, Soil Pollut.* **2013**, *224* (11), 1770.

(4) McLachlan, J. A.; Simpson, E.; Martin, M. Endocrine disrupters and female reproductive health. *Best Pract. Res., Clin. Endocrinol. Metab.* **2006**, *20* (1), 63−75.

(5) Bolong, N.; Ismail, A. F.; Salim, M. R.; Matsuura, T. A review of the effects of emerging contaminants in wastewater and options for their removal. *Desalination* **2009**, *239* (1−3), 229−246.

(6) Trasande, L.; Zoeller, R. T.; Hass, U.; Kortenkamp, A.; Grandjean, P.; Myers, J. P.; DiGangi, J.; Bellanger, M.; Hauser, R.; Legler, J.; Skakkebaek, N. E.; Heindel, J. J. Estimating burden and disease costs of exposure to endocrine-disrupting chemicals in the European Union. *J. Clin. Endocrinol. Metab.* **2015**, *100* (4), 1245−1255.

(7) Semião, A. C.; Schäfer, A. Xenobiotics Removal by Membrane Technology: An Overview. In *Xenobiotics in the Urban Water Cycle*; Fatta-Kassinos, D., Bester, K., Kümmerer, K., Eds.; Environmental Pollution, Vol. *16*; Springer: Dordrecht, The Netherlands, 2009; pp 307−338.

(8) Luo, Y.; Guo, W.; Ngo, H. H.; Nghiem, L. D.; Hai, F. I.; Zhang, J.; Liang, S.; Wang, X. C. A review on the occurrence of micropollutants in the aquatic environment and their fate and removal during wastewater treatment. *Sci. Total Environ.* **2014**, *473−474* (0), 619−641.

(9) Belgiorno, V.; Rizzo, L.; Fatta, D.; Della Rocca, C.; Lofrano, G.; Nikolaou, A.; Naddeo, V.; Meric, S. Review on endocrine disrupting-emerging compounds in urban wastewater: occurrence and removal by photocatalysis and ultrasonic irradiation for wastewater reuse. *Desalination* **2007**, *215* (1−3), 166−176.

(10) Liu, Z.-h.; Ogejo, J. A.; Pruden, A.; Knowlton, K. F. Occurrence, fate and removal of synthetic oral contraceptives (SOCs) in the natural environment: A review. *Sci. Total Environ.* **2011**, *409* (24), 5149−5161.

(11) Braga, O.; Smythe, G.; Schäfer, A.; Feitz, A. Steroid estrogens in ocean sediments. *Chemosphere* **2005**, *61* (6), 827−833.

(12) Onesios, K. M.; Yu, J. T.; Bouwer, E. J. Biodegradation and removal of pharmaceuticals and personal care products in treatment systems: a review. *Biodegradation* **2009**, *20* (4), 441−466.

(13) Pham, T. T.; Nguyen, V. A.; Van der Bruggen, B. Pilot-Scale Evaluation of GAC Adsorption Using Low-Cost, High-Performance Materials for Removal of Pesticides and Organic Matter in Drinking Water Production. *J. Environ. Eng.* **2013**, *139* (7), 958−965.

(14) Pendergast, M. M.; Hoek, E. M. V. A review of water treatment membrane nanotechnologies. *Energy Environ. Sci.* **2011**, *4* (6), 1946−1971.

(15) Shannon, M. A.; Bohn, P. W.; Elimelech, M.; Georgiadis, J. G.; Marinas, B. J.; Mayes, A. M. Science and technology for water purification in the coming decades. *Nature* **2008**, *452* (7185), 301−310.

(16) Kaur, S.; Sundarrajan, S.; Gopal, R.; Ramakrishna, S. Formation and characterization of polyamide composite electrospun nanofibrous membranes for salt separation. *J. Appl. Polym. Sci.* **2012**, *124* (S1), E205−E215.

(17) Ma, Z.; Kotaki, M.; Ramakrishna, S. Surface modified nonwoven polysulphone (PSU) fiber mesh by electrospinning: A novel affinity membrane. *J. Membr. Sci.* **2006**, *272* (1−2), 179−187.

(18) Schiffman, J. D.; Elimelech, M. Antibacterial Activity of Electrospun Polymer Mats with Incorporated Narrow Diameter Single-Walled Carbon Nanotubes. *ACS Appl. Mater. Interfaces* **2011**, *3* (2), 462−468.

(19) Xu, R.; Chi, C.; Li, F.; Zhang, B. Laccase-Polyacrylonitrile Nanofibrous Membrane: Highly Immobilized, Stable, Reusable, and Efficacious for 2,4,6-Trichlorophenol Removal. *ACS Appl. Mater. Interfaces* **2013**, *5* (23), 12554−12560.

(20) Li, X.; Wang, M.; Wang, C.; Cheng, C.; Wang, X. Facile Immobilization of Ag Nanocluster on Nanofibrous Membrane for Oil/Water Separation. *ACS Appl. Mater. Interfaces* **2014**, *6* (17), 15272−15282.

(21) Wu, J.; Wang, N.; Wang, L.; Dong, H.; Zhao, Y.; Jiang, L. Electrospun Porous Structure Fibrous Film with High Oil Adsorption Capacity. *ACS Appl. Mater. Interfaces* **2012**, *4* (6), 3207−3212.

(22) Burger, C.; Hsiao, B. S.; Chu, B. *Annu. Rev. Mater. Res.* **2006**, *36*, 333−368.

(23) Bhardwaj, N.; Kundu, S. C. Electrospinning: A fascinating fiber fabrication technique. *Biotechnol. Adv.* **2010**, *28* (3), 325−347.

(24) Dzenis, Y. Spinning continuous fibers for nanotechnology. *Science* **2004**, *304* (5679), 1917−1919.

(25) Reneker, D. H.; Chun, I. Nanometre diameter fibres of polymer, produced by electrospinning. *Nanotechnology* **1996**, 7 (3), 216.

(26) Shabafrooz, V.; Mozafari, M.; Vashaee, D.; Tayebi, L. Electrospun Nanofibers: From Filtration Membranes to Highly Specialized Tissue Engineering Scaffolds. *J. Nanosci. Nanotechnol.* **2014**, *14* (1), 522−534.

(27) Ma, Z.; Kotaki, M.; Ramakrishna, S. Electrospun cellulose nanofiber as affinity membrane. *J. Membr. Sci.* **2005**, *265* (1−2), 115−123.

(28) Ahmed, F. E.; Lalia, B. S.; Hashaikeh, R. A review on electrospinning for membrane fabrication: challenges and applications. *Desalination* **2015**, *356*, 15−30.

(29) Nasreen, S. A. A. N.; Sundarrajan, S.; Nizar, S. A. S.; Balamurugan, R.; Ramakrishna, S. Advancement in electrospun nanofibrous membranes modification and their application in water treatment. *Membranes* **2013**, *3* (4), 266−284.

(30) Homaeigohar, S. S.; Buhr, K.; Ebert, K. Polyethersulfone electrospun nanofibrous composite membrane for liquid filtration. *J. Membr. Sci.* **2010**, *365* (1), 68−77.

(31) Del Valle, E. M. M. Cyclodextrins and their uses: a review. *Process Biochem.* **2004**, *39* (9), 1033−1046.

(32) Mhlanga, S. D.; Mamba, B. B.; Krause, R. W.; Malefetse, T. J. Removal of organic contaminants from water using nanosponge cyclodextrin polyurethanes. *J. Chem. Technol. Biotechnol.* **2007**, *82* (4), 382−388.

(33) Mbuli, B. S.; Nxumalo, E. N.; Krause, R. W.; Pillay, V. L.; Oren, Y.; Linder, C.; Mamba, B. B. Modification of polyamide thin-film composite membranes with amino-cyclodextrins and diethylamino-cyclodextrins for water desalination. *Sep. Purif. Technol.* **2013**, *120*, 328−340.

(34) Hedges, A. R. Industrial Applications of Cyclodextrins. *Chem. Rev.* **1998**, *98* (5), 2035−2044.

(35) Zolfaghari, G. *β*-Cyclodextrin incorporated nanoporous carbon: Host−guest inclusion for removal of p-Nitrophenol and pesticides from aqueous solutions. *Chem. Eng. J.* **2016**, *283*, 1424−1434.

(36) Crini, G. Recent developments in polysaccharide-based materials used as adsorbents in wastewater treatment. *Prog. Polym. Sci.* **2005**, *30* (1), 38−70.

(37) Adams, F. V.; Nxumalo, E. N.; Krause, R. W. M.; Hoek, E. M. V.; Mamba, B. B. Preparation and characterization of polysulfone/*β*-cyclodextrin polyurethane composite nanofiltration membranes. *J. Membr. Sci.* **2012**, *405–406*, 291−299.

(38) Adams, F. V.; Dlamini, D. S.; Nxumalo, E. N.; Krause, R. W. M.; Hoek, E. M. V.; Mamba, B. B. Solute transport and structural properties of polysulfone/B-cyclodextrin polyurethane mixed-matrix membranes. *J. Membr. Sci.* **2013**, *429*, 58−65.

(39) Adams, F. V.; Nxumalo, E. N.; Krause, R. W. M.; Hoek, E. M. V.; Mamba, B. B. The influence of solvent properties on the performance of polysulfone/*β*-cyclodextrin polyurethane mixed-matrix membranes. *J. Appl. Polym. Sci.* **2013**, *130* (3), 2005−2014.

(40) Adams, F. V.; Nxumalo, E. N.; Krause, R. W. M.; Hoek, E. M. V.; Mamba, B. B. Application of polysulfone/cyclodextrin mixed-matrix membranes in the removal of natural organic matter from water. *Physics and Chemistry of the Earth* **2014**, *67–69*, 71−78.

(41) Alsbaiee, A.; Smith, B. J.; Xiao, L.; Ling, Y.; Helbling, D.; Dichtel, W. R. Rapid removal of organic micropollutants from water by a porous b-cyclodextrin polymer. *Nature* **2016**, *529*, 190−194.

(42) Uyar, T.; Balan, A.; Toppare, L.; Besenbacher, F. Electrospinning of cyclodextrin functionalized poly (methyl methacrylate)-(PMMA) nanofibers. *Polymer* **2009**, *50* (2), 475−480.

(43) Uyar, T.; Havelund, R.; Nur, Y.; Hacaloglu, J.; Besenbacher, F.; Kingshott, P. Molecular filters based on cyclodextrin functionalized electrospun fibers. *J. Membr. Sci.* **2009**, *332* (1−2), 129−137.

(44) Van der Bruggen, B. Integrated Membrane Separation Processes for Recycling of Valuable Wastewater Streams: Nanofiltration, Membrane Distillation, and Membrane Crystallizers Revisited. *Ind. Eng. Chem. Res.* **2013**, *52* (31), 10335−10341.

(45) Luo, Y.; Guo, W.; Ngo, H. H.; Nghiem, L. D.; Hai, F. I.; Zhang, J.; Liang, S.; Wang, X. C. A review on the occurrence of micropollutants in the aquatic environment and their fate and removal during wastewater treatment. *Sci. Total Environ.* **2014**, *473-474*, 619−641.

(46) Semião, A. J.; Schäfer, A. I. Removal of adsorbing estrogenic micropollutants by nanofiltration membranes. Part A—Experimental evidence. *J. Membr. Sci.* **2013**, *431*, 244−256.

(47) Uekama, K.; Fujinaga, T.; Hirayama, F.; Otagiri, M.; Yamasaki, M. Inclusi on complexations of steroid hormones with cyclodextrins in water and in solid phase. *Int. J. Pharm.* **1982**, *10* (1), 1−15.

(48) Bednarek, E.; Bocian, W.; Poznański, J.; Sitkowski, J.; Sadlej-Sosnowska, N.; Kozerski, L. Complexation of steroid hormones: prednisolone, ethinyloestradiol and estriol with *β*-cyclodextrin. An aqueous 1H NMR study. *J. Chem. Soc., Perkin Trans. 2* **2002**, No. 5, 999−1004.

(49) Nagy, Z. M.; Molnár, M.; Fekete-Kertész, I.; Molnár-Perl, I.; Fenyvesi, E.; Gruiz, K. Removal of emerging micropollutants from water using cyclodextrin. *Sci. Total Environ.* **2014**, *485-486*, 711−719.

(50) Rowe, D. R.; Abdel-Magid, I. M. *Handbook of Wastewater Reclamation and Reuse*; CRC Press: Boca Raton, FL, 1995.

(51) Hillis, P. *Membrane Technology in Water and Wastewater Treatment*; Royal Society of Chemistry: Cambridge, U.K., 2000.

(52) Cramer, R. D.; Patterson, D. E.; Bunce, J. D. Comparative Molecular Field Analysis (CoMFA). 1. Effect of Shape on Binding of Steroids to Carrier Proteins. *J. Am. Chem. Soc.* **1988**, *110*, 5959−5967.

(53) Sinha, S. N.; Pal, R.; Dewan, A.; Mansuri, M. M.; Saiyed, H. N. Effect of dissociation energy on ion formation and sensitivity of an analytical method for determination of chlorpyrifos in human blood, using gas chromatography−mass spectrometer (GC−MS in MS/MS). *Int. J. Mass Spectrom.* **2006**, *253* (1−2), 48−57.

(54) Bootharaju, M. S.; Pradeep, T. Understanding the Degradation Pathway of the Pesticide, Chlorpyrifos by Noble Metal Nanoparticles. *Langmuir* **2012**, *28* (5), 2671−2679.

(55) Bailey, H. C.; Deanovic, L.; Reyes, E.; Kimball, T.; Larson, K.; Cortright, K.; Connor, V.; Hinton, D. E. Diazinon and chlorpyrifos in urban waterways in Northern California, USA. *Environ. Toxicol. Chem.* **2000**, *19* (1), 82−87.

(56) Decker, S. P.; Klabunde, J. S.; Khaleel, A.; Klabunde, K. J. Catalyzed Destructive Adsorption of Environmental Toxins with Nanocrystalline Metal Oxides. Fluoro-, Chloro-, Bromocarbons, Sulfur, and Organophosophorus Compounds. *Environ. Sci. Technol.* **2002**, *36* (4), 762−768.

(57) Chang, S.; Waite, T.; Ong, P.; Schäfer, A.; Fane, A. Assessment of Trace Estrogenic Contaminants Removal by Coagulant Addition, Powdered Activated Carbon Adsorption and Powdered Activated Carbon/Microfiltration Processes. *J. Environ. Eng.* **2004**, *130* (7), 736−742.

(58) Food and Agriculture Organization of the United Nations (FAO). Report: CHLORPYRIFOS (017). http://www.fao.org/fileadmin/templates/agphome/documents/Pests_Pesticides/Specs/chlorpyriphos08.pdf (accessed Jan 17, 2018).

(59) Sugaya, Y.; Yoshiba, T.; Kajima, T.; Ishihama, Y. [Development of solubility screening methods in drug discovery]. *Yakugaku Zasshi* **2002**, *122* (3), 237−246.

(60) Yañez, C.; Basualdo, J.; Jara-Ulloa, P.; Squella, J. A. Inclusion complexes of estrone and estradiol with *β*-cyclodextrin: Voltammetric and HPLC studies. *J. Phys. Org. Chem.* **2007**, *20* (7), 499−505.

(61) Mathew, A.; Natarajan, G.; Lehtovaara, L.; Häkkinen, H.; Kumar, R. M.; Subramanian, V.; Jaleel, A.; Pradeep, T. Supramolecular Functionalization and Concomitant Enhancement in Properties of Au25 Clusters. *ACS Nano* **2014**, *8* (1), 139−152.

(62) Negishi, Y.; Nobusada, K.; Tsukuda, T. Glutathione-Protected Gold Clusters Revisited: Bridging the Gap between Gold(I)−Thiolate Complexes and Thiolate-Protected Gold Nanocrystals. *J. Am. Chem. Soc.* **2005**, *127* (14), 5261−5270.

(63) Shibu, E. S.; Pradeep, T. Quantum clusters in cavities: trapped Au15 in cyclodextrins. *Chem. Mater.* **2011**, *23* (4), 989−999.

(64) Mathew, A.; Natarajan, G.; Lehtovaara, L.; Häkkinen, H.; Kumar, R. M.; Subramanian, V.; Jaleel, A.; Pradeep, T. Supramolecular functionalization and concomitant enhancement in properties of Au25 clusters. *ACS Nano* **2014**, *8* (1), 139−152.

(65) Uyar, T.; Besenbacher, F. Electrospinning of cyclodextrin functionalized polyethylene oxide (PEO) nanofibers. *Eur. Polym. J.* **2009**, *45* (4), 1032−1037.

(66) Uyar, T.; Havelund, R.; Hacaloglu, J.; Besenbacher, F.; Kingshott, P. Functional electrospun polystyrene nanofibers incorporating α-, β-, and γ-cyclodextrins: comparison of molecular filter performance. *ACS Nano* **2010**, *4* (9), 5121−5130.

(67) Uyar, T.; Nur, Y.; Hacaloglu, J.; Besenbacher, F. Electrospinning of functional poly (methyl methacrylate) nanofibers containing cyclodextrin-menthol inclusion complexes. *Nanotechnology* **2009**, *20* (12), 125703.

(68) El-Hibri, M. J.; Weinberg, S. A. Polysulfones. In *Encyclopedia of Polymer Science and Technology*; John Wiley & Sons: New York, 2011; Vol. *4*, pp 1−26.

(69) Kaur, S.; Sundarrajan, S.; Rana, D.; Sridhar, R.; Gopal, R.; Matsuura, T.; Ramakrishna, S. Review: the characterization of electrospun nanofibrous liquid filtration membranes. *J. Mater. Sci.* **2014**, *49* (18), 6143−6159.

(70) Armenta, S.; Quintás, G.; Garrigues, S.; de la Guardia, M. A validated and fast procedure for FTIR determination of Cypermethrin and Chlorpyrifos. *Talanta* **2005**, *67* (3), 634−639.